Influence of titanium on structure formation, liquation processes and microhardness of structural components of Al – Ni – Ti alloys synthesized from the oxide phases by SHS metallurgy

E. H. Ri, *Dr. Eng., Prof., Head of the Department of Foundry Engineering and Metal Technology*[1], *e-mail: erikri999@mail.ru*
Hosen Ri, *Dr. Eng., Prof.*[1], *e-mail: opirus@bk.ru*
K. V. Doroshenko, *Post-graduate Student of the Department of Foundry and Metal Technology*[1], *e-mail: rbhbkk1212@yandex.ru*
E. V. Kim, *Senior Lecturer of the Department of Foundry Engineering and Metal Technology*[1], *e-mail: jenya_1992g@mail.ru*

[1]*Federal State Budgetary Educational Institution of Higher Education "Pacific National University", Khabarovsk, Russia.*

The paper is devoted to revealing the regularities of the influence of titanium (0.91, 2.42, 3.19, 3.39, 4.32 and 8.81 wt.%) on structure formation, nature of element distribution and microhardness of structural components in Al – Ni – Ti alloys by aluminothermy during SHS metallurgy. As the initial composition of the charge were selected the following materials in fractional parts: Al:NiO_2:CaF_2:$NaNO_3$:TiO_2 = 10:10:12:6:*X*, where *X* = 1.5, 4.5, 5.0, 7.0, 10.0.
The structural components in Al – Ni – Ti alloys have been identified by electron microscopy and *X*-ray spectral analysis of elements. In the alloys with 0.91–4.32 wt.% Ti the following phases crystallize: β′-phase (solid solution of Ni in the nickel aluminide AlNi) Al_3Ni_2, Al_3Ti, Al_3Ni and α-solid solution of Ni and Ti in aluminum. In an alloy with 8.81 wt.% Ti the β′-phase turns into a titanium-doped nickel aluminide Al(NiTi) (composition in at.%: 50.53 Al; 1.47 Ti; 48.0 Ni). The increase of titanium content in Al – Ni – Ti alloys increases the solubility of Ni in the β′-phase and at titanium concentration in the alloy 8.81 wt.% in the aluminide Al(NiTi) up to 48 at.% Ni is dissolved compared to the solubility of nickel (38 at.%) in the alloy with 0.91 wt.% Ti. Increasing the nickel content in the above phases contributes to their microhardness from 13 GPa to 14.8 GPa at 8.81 wt.% Ti.
Increasing the titanium content in Al – Ni – Ti alloys to 4.32 wt.% increases the solubility of nickel in the nickel aluminide Al_3Ni, with a higher concentration of titanium (8.81 wt.%) in the nickel aluminide with titanium Al(NiTi) dissolves up to 48.53 at.% Ni, while in the alloy with 0.91 wt.% Ti – only about 1.0 at.% Ni. At the same time, the Al and Ti content in titanium aluminide Al_3Ti decreases and its microhardness increases. It was not possible to determine the microhardness of Al(NiTi) aluminide because of the formation of a porous structure.
In nickel aluminide Al_3Ni, an increase in titanium content leads to an increase in nickel concentration to 4.32 wt.% Ti followed by a slight increase to 8.81 wt.% Ti. Despite increasing the nickel content and decreasing the aluminum concentration, the microhardness of the nickel aluminide decreases. Apparently, this circumstance is caused by the formation of a porous structure in this phase.

Key words: alloy, microhardness, concentration, aluminides, solubility, liquation, solid solution.
DOI: 10.17580/nfm.2022.01.06

Introduction

Nickel-based superalloys with excellent mechanical properties (for example, strength of creep and impact strength) and excellent resistance to oxidation and corrosion are prospective metallic materials for high-temperature applications such as turbine blades and nuclear reactors. In this unique class of materials, L12-type γ′-Ni_3Al ordered precipitates, having a volume fraction of ≈ 0.7, are coherently distributed in a disordered FCC-type γ-Ni matrix and prevent dislocation movement under severe creep conditions. [1–2] Over the past few decades, to further improve the performance of Ni-based superalloys at elevated operating temperatures, much research has focused on the development of advanced manufacturing techniques (for example, Bridgman solidification of single crystals [2–5]) and processing techniques (for example, additive manufacturing using laser [6–8]). Nevertheless, defects related to geometry, undirected grains, porosities, and microcracks caused by these fabrication techniques strongly hinder the mass production of large components with complex morphologies. [2–3, 5–7] On the other hand, microstructural manipulation of conventional polycrystalline superalloys through the addition of refractory alloying elements has always been an alternative in alloy design to ensure the phase stability of γ′-precipitation. In this context, it has been reported that impurity atoms of Cr, Mo, W, and Re restrain the creep rupture, slowing down the kinetics of the enlargement of the γ′ phase. [9–15] Moreover, Van Sleitman and Pollock [16] stated that the best creep

resistance of Ni-based superalloys can be obtained when the lattice mismatch δ between γ′ and γ phases is almost 0.4%, i. e., $|\delta| \approx 0.4\%$. the parameter δ is defined as [1–2]

$$\delta = 2 \cdot \frac{a_{\gamma'} - a_{\gamma}}{a_{\gamma'} - a_{\gamma}}$$

where $a_{\gamma'}$ and a_{γ} are the lattice parameters of γ′-and γ-phases.

It has been established that the value |δ|, which determines the characteristics of the shape of γ′ intermetallics, is determined by elastic stresses. If $|\delta| = 0$, full consistency is established around tiny spherical γ′ precipitation in the early stages of exposure to high temperatures, while in the later stages, distinct-shaped γ′ precipitation is formed (for example spherical → spheroidal → cubic ($|\delta| \approx 0.4\%$) → → cubic → irregular ($|\delta| > 1\ \%$)) [16–19]. For this reason, the atomic positions of various types of refractory impurities in the γ′ and γ phases (for example their preferences in phase and location) not only preserve the microstructural stability of the constituent phases by adjusting the parameter |δ| to its ideal value, but also take part in strengthening the bonds [20–22].

An example of the above conditions is the Ni – Al – Ti system, as the main subsystem of a nickel-based alloy, widely used in the aerospace and energy industries due to its high strength and excellent corrosion resistance at high temperatures [23–26]. Even though the Ni – Al – Ti system is a key metal material used in various industries, data on the high–order system is still incomplete compared to data on binary systems such as Ni – Al, Ni – Ti and Al – Ti. At the same time, the high cost of production is one of the main constraining factors for the widespread use of composite materials in industrial production.

One of the ways to solve the problem of finding a promising and economically feasible technology for producing NiAl can be self-propagating high-temperature synthesis (SHS) [27]. The SHS method can be divided into several varieties: according to the composition of charge materials (metals or their oxides), the type of reducing agents (Al, Mg, Ca, etc.), the phase composition of the product after a metallothermic reaction (solid or liquid phase). The SHS process using a charge in the form of oxides has certain advantages, in which a metallothermic reaction occurs with the formation of a product in the form of a liquid phase. This makes it possible to use the SHS process to obtain a hardening phase inside a metal matrix alloy. Nickel aluminides are obtained by the SHS method, which are used as a basis in modern composite materials. The high temperature developing in thermite processes, which is difficult to achieve by conventional heating, makes it possible to obtain cast composite materials according to a short scheme [28–35].

The use of metallothermic processes is economically feasible in the production of intermetallic alloys through the joint reduction of thermodynamically stable metal oxides [36–39]. The present study is a development of the work [36], where the Ti content in the Al – Ni – Ti alloy varied from 0 to 8.81 wt.%.

Thus, the objective of this study is to obtain titanium-doped nickel aluminides during their synthesis from nickel and titanium oxide compounds by the method of SHS metallurgy, as well as to study the effect of titanium on structure formation, liquation processes and microhardness of the structural components of the Al – Ni – Ti alloy.

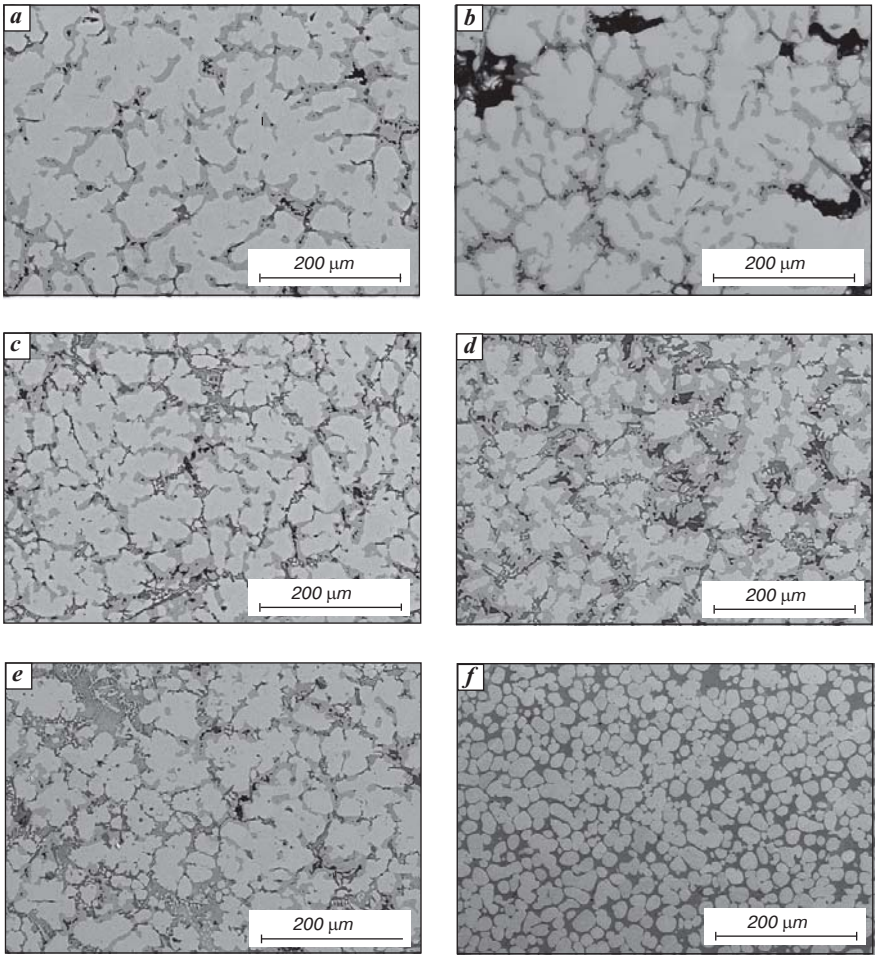

Fig. 1. Microstructure of Al – Ni – Ti alloys in reflected electrons on a scanning electron microscope (SEM) at various magnifications:
a — 0.91 wt.% Ti; *b* — 2.42 wt.% Ti; *c* — 3.19 wt.% Ti; *d* — 3.39 wt.% Ti; *e* — 4.32 wt.% Ti; *f* – 8.81 wt.% Ti

Research methods and materials

The starting materials were nickel oxide NiO_2 (99.5 wt.%, TU 6-09-3642-74), TiO_2 (99.5 wt.% STP TU COMP 2-340-11), sodium nitrate (GOST 4168-79), calcium fluoride CaF_2 (98.0 wt.%, TU 2621-007-69886968-2015 with ed. 1) and aluminum powder (98.0 wt.%, PA-4 GOST 6058-73).

For the successful implementation of the joint reduction process, an increase in the thermal effect is required due to the weak efficiency of the titanium oxide reduction reaction. Therefore, a thermite additive of sodium nitrate $NaNO_3$ is introduced into the charge. The introduction of $NaNO_3$ into the metallothermite mixture leads to an increase in the thermal effect sufficient to melt the reaction products and separate them into a metallic and slag phase. Sodium nitrate, when interacting with aluminum, decomposes by the reaction of $6NaNO_3 + 10Al = 3Na_2O + 3N_2 + 5Al_2O_3$ with the release of nitrogen. Reduced titanium, reacting with nitrogen, forms nitride by the reaction $2Ti + N_2 = 2TiN$ ($\Delta G \approx 300–320$ kJ/mol). The reaction is exothermic and is accompanied by significant heat release. Calcium fluoride CaF_2 (~15 wt.%) was used as a flux.

The following modern research methods were used:

– *X*-ray spectral analysis to determine the content of elements in various structural components of alloys was performed at the analytical research complex, based on FE-SEM Hitachi SU-70 (Japan) with energy dispersive (Thermo Scientific Ultra Dry) and wave (Thermo Scientific Magna Ray) prefixes of reflected electron diffraction Instruments HKL Nordlys;

– microhardness tests (H_{50}) were carried out according to the standard procedure on the Shimadzu HMV-G21DT device.

Main results and their discussion

The initial composition of the charge in fractional parts for the obtained alloys

Al – Ni – Ti is the following: Al : NiO_2 : CaF_2 : $NaNO_3$: TiO_2 = 10 : 10 : 12 : 6 : *X*, where *X* = 1.5, 4.5, 5.0, 7.0, 10.0.

The Ti content in Al – Ni – Ti alloys varies within the following limits: 0.91, 2.42, 3.19, 3.39, 4.32, 8.81 wt.% Ti. At the same time, the content of Al and Ni ranges from 41.0-51.0 wt.% Al and 43-47 wt.% Ni, and the concentration of Fe is 0.13-0.22 wt.%.

With an increase in the titanium content, a change in the structural components is observed (**Fig. 1**). With a high content of Ti (8.81 wt.%) spheroidization of intermetallic occurs (**Fig. 1, *f***).

Let us consider in more detail the processes of structure formation and liquation of elements in structural components in alloys with 0.91 (**Fig. 2, *a-c***) and 8.81 wt.% Ti (**Fig. 3, *a-c***).

In the alloy Al – Ni – 0.91 wt.% Ti the following phases crystallize:

1. At points 1-3, the β′-phase crystallizes (a solid solution of Ni in AlNi aluminide, the left part relative to the singular melting point of AlNi), which has a white hue and is the main phase in the Al – Ni – Ti alloy.

2. At points 4-6, nickel aluminide Al_3Ni crystallizes, in the form of a compact polyhedron shape with dimensions of about 25 μm. It has a light gray color.

3. At points 7-9, titanium aluminide Al_3Ti is observed, having a dark gray shade and an oblong shape, crystallizes between the grains of the β′ phase, as well as nickel aluminide Al_3Ni.

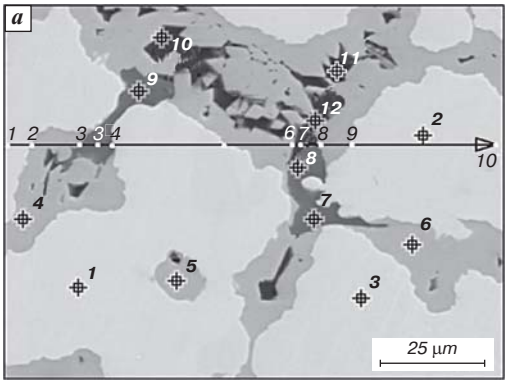

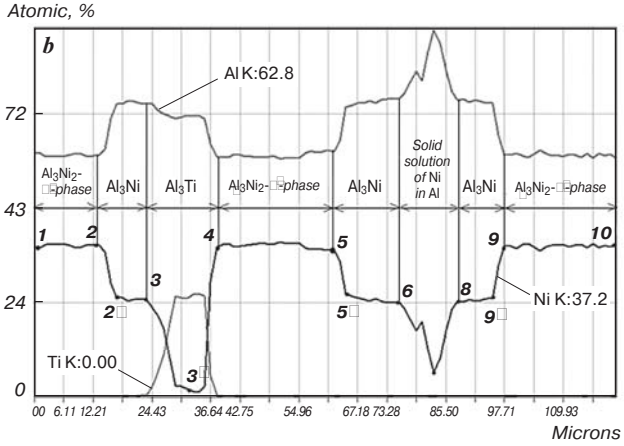

Analysis points of elements	The structural components	The content of the elements, at.%				
		Al	Si	Ti	Fe	Ni
1-3	The β′-phase - a solid solution of Ni in AlNi aluminide	61.16	–	–	–	38.84
		$Al_{61.16}Ni_{38.84} = Al_{1,6}Ni$ = β-phase or $Al_{3.2}Ni_2 \approx Al_3Ni_2$				
4-6	Nickel aluminide Al_3Ni	74.88	–	–	0.26	24.86
		$Al_{74.88}Ni_{24.86} = Al_{3.01}Ni \approx Al_3Ni$				
7-9	Titanium aluminide Al_3Ti	71.53	0.74	26.66	–	1.07
		$Al_{71.53}Ti_{26.66} = Al2.68Ti \approx Al_3Ti$				
10-12	α- solid solution of Ni and Ti in Al	98.39	–	0.1	–	1.51

c

Fig. 2. Microstructure, analysis points of elements (*a*), their distribution in structural components (*b* and *c*) of Al – Ni – Ti alloy with 0.91 wt.% Ti

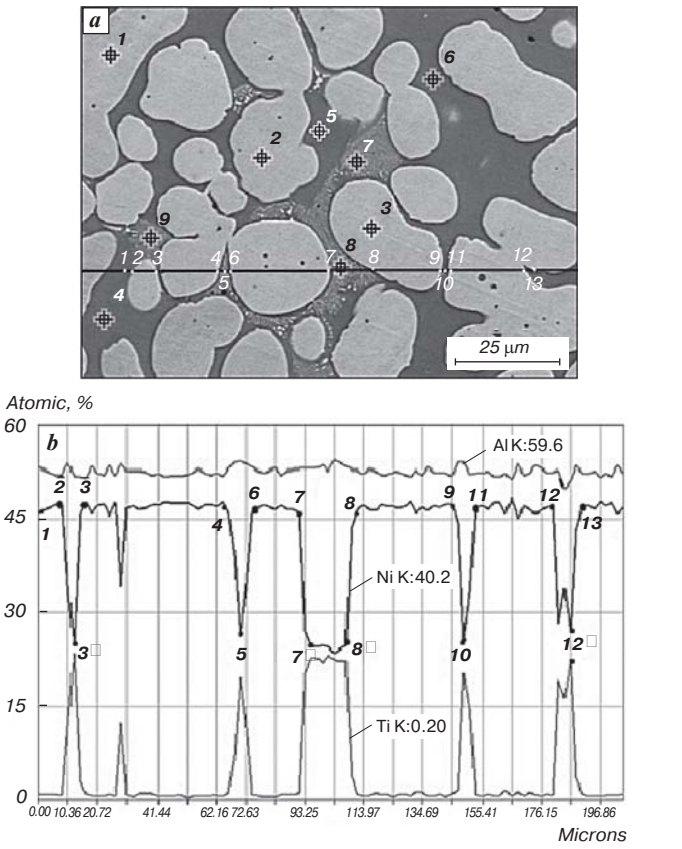

Analysis points of elements	The structural components	The content of the elements, at.%		
		Al	Ti	Ni
1-3	Nickel aluminides with titanium Al(Ni, Ti)	50.53	1.47	48.0
		$Al_{50.53}(Ni, Ti) = Al_{1.02}(Ni, Ti) \approx Al(Ni, Ti)$		
4-6	Nickel and titanium aluminide Al_2NiTi	50.0	24.6	25.4
		$Al_{50.0}Ni_{25.4}Ti_{24.6} = Al_2Ni_{1.03}Ti \approx Al_2NiTi$		
7-9	Nickel and titanium aluminide Al_2NiTi	47.3	24.17	28.53
		$Al_{47.3}Ni_{28.53}Ti_{24.17} = Al_{1.95}Ni_{1.18}Ti \approx Al_2NiTi$		

Fig. 3. Microstructure, analysis points of elements (*a*), their distribution in structural components (*b* and *c*) of Al – Ni – Ti alloy with 8.81 wt.% Ti

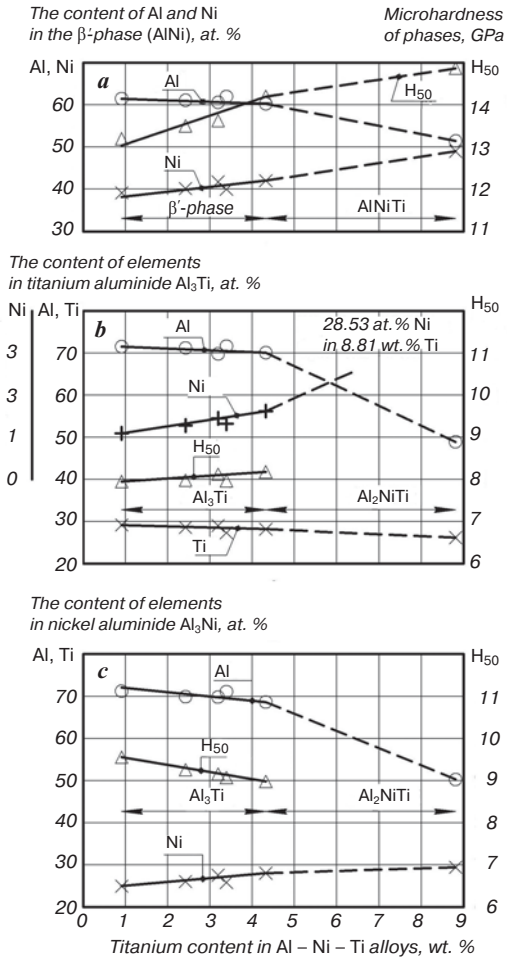

Fig. 4. Effect of titanium on the solubility of elements and microhardness of structural components of Al – Ni – Ti alloys

4. In dark inclusions (points 10-12), a solid solution of Ni and Ti in aluminum crystallizes. Titanium does not always dissolve in Al, but an α-solid solution without titanium is often observed.

The presence of the above structural components is confirmed by the curves of the distribution of elements in the structural components of the Al – Ni – Ti alloy with 0.91 wt.% Ti in the direction of profile A-A (Fig. 2, *b*).

Thus, in the Al – Ni – Ti alloy (0.91 wt.% Ti), the structure consists of a basic β′ phase, a small amount of titanium and nickel aluminides (Al_3Ti, Al_3Ni) and an α-solid nickel solution in aluminum. Titanium is sometimes dissolved in it up to 0.3 at.%.

In the Al – Ni – Ti alloy (8.81 wt.% Ti), the structural components are (Fig. 3, *a-c*):

1. Nickel aluminides with titanium (1.47 at.%), having a light shade and compact shape in the form of spherical inclusions and occupies a large area on the shelf (points 1-3). Stoichiometry: $Al_{50.53}(Ni, Ti)_{49.5} = Al_{1.02}(Ni, Ti) \approx Al(Ni, Ti)$.

2. Nickel and titanium aluminide (points 4-6), having a black hue and located between the grains of nickel aluminide (points 1-3). Stoichiometry: $Al_{50.0}Ni_{25.4}Ti_{24.6} = Al_2Ni_{1.03}Ti \approx Al_2NiTi$.

3. Nickel and titanium aluminide (points 7-9) is located against the background of a similar aluminide, but with a higher concentration of Ni (28.53 at.%) compared to the previous aluminide (25.4 at.%). The grains are light gray in color and small. Stoichiometry: $Al_{47.3}Ni_{28.53}Ti_{24.17} = Al_{1.95}Ni_{1.18}Ti \approx Al_2NiTi$.

It was found that at low titanium contents (0.91-4.32 wt.%), Al_3Ni_2 (β′-phase solid solution of Ni in AlNi aluminide) crystallizes in Al – Ni – Ti alloys. With a higher titanium content (8.81 wt.%), the β′-phase is converted into titanium-doped nickel aluminide Al(Ni, Ti), composition in at.%: 50.53 Al; 1.47 Ti; 48.0 Ni.

With an increase in the titanium content, the solubility of nickel in the β′ phase also increases at a concentration of 8.81 wt.% Ti in Al(Ni, Ti) aluminide dissolves to 48 at.% compared to the solubility of nickel 38.84 at.% in Al – Ni – Ti alloy (0.91 wt.%). An increase in the

nickel content in the above phases contributes to an increase in their microhardness **(Fig. 4, *a*)**.

Titanium (Al_3Ti) and nickel (Al_3Ni) aluminides crystallize in alloys with a titanium content from 0.91 to 4.32 wt.%. With a high titanium content (8.81 wt.%), these aluminides turn into titanium-doped aluminide Al_2NiTi, the average composition in at.%: 47.3-50.0 Al; 25.4-28.53 Ni; 24.17-24.6 Ti.

As can be seen from **Fig. 4, *b***, an increase in the titanium content contributes to an increase in the nickel content in titanium aluminide Al_3Ti. At the same time, the content of Al and Ti decreases, and the microhardness increases slightly. With a high titanium content (8.81 wt.%) in the Al – Ni – Ti alloy, the Ni concentration increases to 28.53 at.%, and the solubility of titanium monotonically decreases. It was not possible to determine the microhardness of the Al_2NiTi phase.

In nickel aluminide (Al_3Ni), an increase in the titanium content leads to a slight increase in the Ni concentration to 4.32 wt.% Ti. The nickel content in Al_2NiTi aluminide nearly does not change **(Fig. 4, *c*)**. Despite a slight increase in the Ni content, the microhardness of Al_3Ni aluminide decreases.

Conclusions

1. With an increase in the titanium content, the structural components of Al – Ni – Ti alloys are crushed and their spheroidization is observed, this is especially noticeable in an alloy with a high titanium content (8.81 wt.%).

2. The structural components in Al – Ni – Ti alloys with different titanium content have been identified by electron microscopy and *X*-ray spectral analysis of elements (0.91, 2.42, 3.19, 3.39 4.32, 8.81 wt.%):

– in Al – Ni – Ti alloys from 0.91 to 4.32 wt.% Ti inclusive, the main structural components are the β′-phase (Al_3Ni_2), Al_3Ni, Al_3Ti and α-a solid solution of Ni and Ti in aluminum;

– with a high titanium content (8.81 wt.%), the β′-phase turns into titanium-doped nickel aluminide Al(NiTi) (composition in at.%: 50.53 Al; 1.47 Ti; 48.0 Ni), and the aluminides Al_3Ni and Al_3Ti – into titanium-doped nickel aluminide Al_2NiTi (composition in at.%: 47.3-50.0 Al; 25.4-28.53 Ni; 24.17–24.6 Ti);

– The α-solid solution of Ni and Ti in Al disappears.

3. With an increase in the titanium content to 4.32 wt.%, the solubility of Ni in the β′ phase also increases at a concentration of 8.81 wt.% Ti it reaches 48 at.% (38 at.% Ni at 0.91 wt.% Ti). At the same time, the microhardness of the β′-phase and nickel aluminide Al(NiTi) increases.

4. An increase in the Ti content in Al – Ni – Ti alloys (from 0.91 to 4.32 wt.%) contributes to an increase in the solubility of Ni and the microhardness of titanium aluminide Al_3Ti. At the same time, the content of Al and Ti decreases.

With a high Ti content in the Al – Ni – Ti alloy (8.81 wt %), the solubility of Ni in this phase reaches up to 48.0 at.% (38 at.% Ni at 0.91 wt.% Ti).

5. An increase in the Ti content in Al – Ni – Ti alloys (from 0.91 to 4.32 wt.%) leads to a slight increase in the solubility of Ni in nickel aluminide Al_3Ni and a decrease in the concentration of Al. The microhardness decreases at the same time, which is due to the formation of microporosity in Al_3Ni crystals. With a higher concentration of titanium (8.81 wt.%), the Ni content reaches up to 28.53 at.% (24.86 at.% Ni at 0.91 wt.% Ti), and aluminum – up to 50 at.% (75 at.% at. 0.91 wt.% Ti). Microhardness was not determined due to the formation of a porous structure in Al_3Ni aluminide.

The research was carried out at the Center for Collective Use "Applied Materials Science" of the Federal State Budgetary Educational Institution of Higher Education "TOGU" with the financial support of the Ministry of Science and Education of the Russian Federation within the framework of research work No state reg. of the state task AAAA-A20-120021490002-1.

References

1. Reed R. C. The Superalloys: Fundamentals and Applications. 1st ed. Cambridge: Cambridge University Press, 2006. xv+372 p.

2. Pollock T. M., Tin S. Nickel-Based Superalloys for Advanced Turbine Engines: Chemistry, Microstructure and Properties. *Journal of Propulsion and Power*. 2006. Vol. 22, Iss. 2. pp. 361–374.

3. Ma D. Novel Casting Processes for Single-Crystal Turbine Blades of Superalloys. *Frontiers of Mechanical Engineering*. 2018. Vol. 13, Iss. 1. pp. 3–16.

4. Wang F., Ma D., Zhang J., Liu L., Bogner S., Bührig-Polaczek A. Effect of Local Cooling Rates on the Microstructures of Single Crystal CMSX-6 Superalloy: a Comparative Assessment of the Bridgman and the Downward Directional Solidification Processes. *Journal of Alloys and Compounds*. 2014. Vol. 616. pp. 102–109.

5. Elliott A. J., Pollock T. M., Tin S., King W. T., Huang S.-C., Gigliotti M. F. X. Directional Solidification of Large Superalloy Castings with Radiation and Liquid-Metal Cooling: a Comparative Assessment. *Metallurgical and Materials Transactions A*. 2004. Vol. 35, Iss. 10. pp. 3221–3231.

6. Qi H., Azer M., Ritter A. Studies of Standard Heat Treatment Effects on Microstructure and Mechanical Properties of Laser Net Shape Manufactured Inconel 718. *Metallurgical and Materials Transactions A*. 2009. Vol. 40, Iss. 10. pp. 2410–2422.

7. Harrison N. J., Todd I., Mumtaz K. Reduction of Micro-Cracking in Nickel Superalloys Processed by Selective Laser Melting: a Fundamental Alloy Design Approach. *Acta Materialia*. 2015. Vol. 94. pp. 59–68.

8. Bi G., Sun C.-N., Chen H.-C., Ng F. N., Ma C. C. K. Microstructure and Tensile Properties of Superalloy IN100 Fabricated by Micro-Laser Aided Additive Manufacturing. *Materials & Design*. 2014. Vol. 60. pp. 401–408.

9. Ng D. S., Chung D.-W., Toinin J. P., Seidman D. N., Dunand D. C., Lass E. A. Effect of Cr Additions on a γ-γ′ Microstructure and Creep Behavior of a Co-based Superalloy with Low W Content. *Materials Science and Engineering: A*. 2020. Vol. 778. 139108. DOI: 10.1016/j.msea.2020.139108

10. Tu Y., Mao Z., Seidman D. N. Phase-Partitioning and Site-Substitution Patterns of Molybdenum in a Model Ni –Al – Mo Superalloy: an Atom-Probe Tomographic and First-Principles Study. *Applied Physics Letters*. 2012. Vol. 101, Iss. 12. 121910. DOI: 10.1063/1.4753929

11. Fährmann M., Fratzl P., Paris O., Fährmann E., Johnson W. C. Influence of Coherency Stress on Microstructural Evolution in Model Ni–Al–Mo Alloys. *Acta metallurgica et Materialia*. 1995. Vol. 43, Iss. 3. pp. 1007–1022.

12. Tian S., Zeng Z., Fushun L., Zhang C., Liu C. Creep Behavior of a 4.5%-Re Single Crystal Nickel-Based Superalloy at Intermediate Temperatures. *Materials Science and Engineering: A*. 2012. Vol. 543. pp. 104–109.

13. Wöllmer S., Mack T., Glatzel U. Influence of Tungsten and Rhenium Concentration on Creep Properties of a Second Generation Superalloy. *Materials Science and Engineering: A*. 2001. Vol. 319. pp. 792–795.

14. Sudbrack C. K., Isheim D., Noebe R. D., Jacobson N. S., Seidman D. N. The Influence of Tungsten on the Chemical Composition of a Temporally Evolving Nanostructure of a Model Ni – Al – Cr Superalloy. *Microscopy and Microanalysis*. 2004. Vol. 10, No. 3. pp. 355–365.

15. Wang T., Sheng G., Liu Z.-K., Chen L.-Q. Coarsening Kinetics of γ′ Precipitates in the Ni–Al–Mo System. *Acta Materialia*. 2008. Vol. 56, Iss. 19. pp. 5544–5551.

16. van Sluytman J. S., Pollock T. M. Optimal Precipitate Shapes in Nickel-Base γ–γ′ Alloys. *Acta Materialia*. 2012. Vol. 60, Iss. 4. pp. 1771–1783.

17. Eriş R., Akdeniz M. V., Mekhrabov A. O. Atomic Size Effect of Alloying Elements on the Formation, Evolution and Strengthening of γ′-Ni_3Al Precipitates in Ni-Based Superalloys. *Intermetallics*. 2019. Vol. 109. pp. 37–47.

18. Hisazawa H., Terada Y., Takeyama M. Morphology Evolution of γ′ Precipitates During Isothermal Exposure in Wrought Ni-Based Superalloy Inconel X-750. *Materials Transactions*. 2017. Vol. 58, Iss. 5. pp. 817–824.

19. Bocchini P. J., Sudbrack C. K., Noebe R. D., Seidman D. N. Temporal Evolution of a Model Co–Al–W Superalloy Aged at 650° C and 750° C. *Acta Materialia*. 2018. Vol. 159. pp. 197–208.

20. Long H., Mao S., Liu Y., Zhang Z., Han X. Microstructural and Compositional Design of Ni-Based Single Crystalline Superalloys — A review. *Journal of Alloys and Compounds*. 2018. Vol. 743. pp. 203–220.

21. Van Sluytman J. S., Moceri C. J., Pollock T. M. A Pt-Modified Ni-Base Superalloy with High Temperature Precipitate Stability. *Materials Science and Engineering: A*. 2015. Vol. 639. pp. 747–754.

22. Eriş R., Akdeniz M. V., Mekhrabov A. O. The Site Preferences of Transition Elements and Their Synergistic Effects on the Bonding Strengthening and Structural Stability of γ′-Ni3Al Precipitates in Ni-Based Superalloys: a First-Principles Investigation. *Metallurgical and Materials Transactions A*. 2021. Vol. 52, Iss. 6. pp. 2298–2313.

23. Choudhury I. A., El-Baradie M. A. Machinability of Nickel-Base Super Alloys: a General Review. *Journal of Materials Processing Technology*. 1998. Vol. 77, Iss. 1–3. pp. 278–284.

24. Loria E. A. Recent developments in the progress of superalloy 718. *JOM*. 1992. Vol. 44, Iss. 6. pp. 33–36.

25. Meetham G. W. High-temperature materials — a general review. *Journal of Materials Science*. 1991. Vol. 26, Iss. 4. pp. 853–860.

26. Njah N., Dimitrov O. Microstructural evolution of nickel-rich Ni–Al–Ti alloys during aging treatments: the effect of composition. *Acta Metallurgica*. 1989. Vol. 37, Iss. 9. pp. 2559–2566.

27. Prusov E. S., Panfilov A. A., Kechin V. A. Role of powder precursors in production of composite alloys using liquid-phase methods. *Russian Journal of Non-Ferrous Metals*. 2017. Vol. 58, Iss. 3. pp. 308–316.

28. Sanin V., Andreev D., Ikornikov D., Yukhvid V. Cast Intermetallic Alloys by SHS Under High Gravity. *Acta Physica Polonica: A*. 2011. Vol. 120, Iss. 2. pp. 331–335.

29. Amosov A. P., Lutz A. R., Latukhin E. I., Eroshkin A. A. Application of SHS Processes for The Production of in Situ Aluminum Matrix Composites Discretely Reinforced with Nanosized Titanium Carbide Particles. Review. *Izvestiya Vuzov. Tsvetnaya Metallurgiya*. 2016. No. 1. pp. 39–49.

30. Tiwary C., Gunjal V., Banerjee D., Chattopadhyay K. Intermetallic Eutectic Alloys in the Ni – Al – Zr System with Attractive High Temperature Properties. *MATEC Web of Conferences*. 2014. Vol. 14. 01005. DOI: 10.1051/matecconf/20141401005

31. Fukumoto M., Yokota T., Hara M. Formation of Ni Aluminide Containing Zr by Synchronous Electrodeposition of Al and Zr and Cyclic-Oxidation Resistance. *Journal of the Japan Institute of Metals*. 2010. Vol. 74, Iss. 9. pp. 584–591.

32. Wang L., Yao Ch., Shen J., Zhang Yu. Microstructures and Compressive Properties of NiAl – Cr (Mo) and NiAl – Cr Eutectic Alloys with Different Fe Contents. *Materials Science and Engineering: A*. 2019. Vol. 744. pp. 593–603.

33. Levashov E. A. Promising Materials and Technologies of Self-Propagating High-Temperature Synthesis. Moscow : Izdatelskiy dom "MISiS", 2011. 378 p.

34. Parsa M. R., Soltanieh M. On the Formation of Al3Ni2 Intermetallic Compound by Aluminothermic Reduction of Nickel Oxide. *Materials Characterization*. 2011. Vol. 62, Iss. 7. pp. 691–696.

35. Khimukhin S. N., Kim E. D., Ri E. H. Synthesis of NiAl Composite Alloys by Metallothermy Method. *Materials Today: Proceedings*. 2019. Vol. 19. pp. 2278–2282.

36. Gostishchev V., Ri E., Ri H., Kim E., Ermakov M., Khimukhin S., Deev V., Prusov E. Synthesis of Complex-Alloyed Nickel Aluminides from Oxide Compounds by Aluminothermic Method. *Metals*. 2018. Vol. 8, Iss. 6. p. 439.

37. Ri Hosen, Gostishchev V. V., Ri E. H., Khimukhin S. N., Kim E. D., Medneva A. V. Development of the Synthesis Technology of Doped Nickel Aluminides From Oxide Compoumds by Aluminothermic Method. *Metallurgia Mashinostroyeniya*. 2018. No. 1. pp. 30–35.

38. Bazhin V. Y., Kosov Y. I., Lobacheva O. L., Dzhevaga N. V. Synthesis of Aluminum-Based Scandium–Yttrium Master Alloys. *Russian Metallurgy (Metally)*. 2015. Vol. 2015, Iss. 7. pp. 516–520.

39. Khimukhin S. N., Kim E. D., Ri E. H. Synthesis of NiAl Composite Alloys by Metallothermy Method. *Materials Today: Proceedings*. 2019. Vol. 19. pp. 2278–2282.

NFM